Spatial sensitivity of human circadian response: Melatonin suppression from on-axis and off-axis light exposures

Rohan Nagare, Mark S. Rea [*], Mariana G. Figueiro

Light and Health Research Center, Department of Population Health Science and Policy, Icahn School of Medicine at Mount Sinai, New York, NY, USA

ARTICLE INFO

ABSTRACT

A better understanding of the spatial sensitivity of the human circadian system to photic stimulation can provide practical solutions for optimized circadian light exposures. Two psychophysical experiments, involving 25 adult participants in Experiment 1 (mean age = 34.0 years [SD 15.5]; 13 females) and 15 adult participants in Experiment 2 (mean age = 43.0 years [SD 12.6]; 12 females), were designed to investigate whether varying only the spatial distribution of luminous stimuli in the environment while maintaining a constant spectrally weighted irradiance at the eye could influence nocturnal melatonin suppression. Two spatial distributions were employed, one where the luminous stimulus was presented On-axis (along the line of sight) and one where two luminous stimuli were both presented Off-axis (laterally displaced at center by 14°). Two narrowband LED light sources, blue (λ_{max} = 451 nm) for first experiment and green (λ_{max} = 522 nm) for second experiment, were used in both the On-axis and the Off-axis spatial distributions. The blue luminous stimulus targeting the fovea and parafovea (On-axis) was about three times more effective for suppressing melatonin than the photometrically and spectrally matched stimulus targeting the more peripheral retina (Off-axis). The green luminous stimulus targeting the fovea and parafovea (On-axis) was about two times more effective for suppressing melatonin than the photometrically and spectrally matched stimulus targeting the more peripheral retina (Off-axis).

1. Introduction

Much has already been discovered regarding the spectral, absolute, and temporal sensitivities of circadian phototransduction as characterized by light-induced melatonin suppression (Brainard et al., 2001; Khalsa et al., 2003; St Hilaire et al., 2012; Thapan et al., 2001; Zeitzer et al., 2000). For instance, it is now known that the human circadian system is most sensitive to short-wavelength light (circa 460 nm) (Brainard et al., 2001; Thapan et al., 2001) and that a greater amount of light is required to influence nighttime melatonin levels than that required to read black text on white paper (Zeitzer et al., 2000). Further, exposure to the same spectrum and amount can advance or delay the biological clock, depending upon the time of exposure. However, much less is known about the spatial distribution of the luminous elements in the environment that affect human circadian response.

Anisotropic distributions of retinal neurons, including photoreceptors, across the inner surface of the eye (Bumsted and Hendrickson, 1999; Calkins, 2001; Curcio and Allen, 1990; Curcio et al., 1990; Lee et al., 2019; Nasir-Ahmad et al., 2017; Watson, 2014; Wells-Gray et al.,

2016), have been shown to influence human visual responses. For instance (Fig. 1), the greater density of cones with very small, overlapping receptive fields in the foveola (angular diameter ≈ 1°20') provide humans with high, On-axis, spatial resolution (Kolb et al., 2020). An increase in radial eccentricity beyond the foveola is marked by significantly reduced cone density and larger receptive fields, which reduces Off-axis spatial resolution. More proximal neurons involved in circadian phototransduction, intrinsically photosensitive retinal ganglion cells (ipRGCs) as well as bipolar and amacrine cells, are found throughout the retina *except in the foveola*, but have their highest density in and around the macula (angular diameter ≈ 8° to 12°). Hannibal et al. (2017), for example, showed the highest density of ipRGC cell bodies in human retinae are located near the fovea (angular diameter ≈ 5°) and Nasir-Ahmad et al. (2017) showed the highest density of ipRGCs to be located within the parafovea (angular concentric extent from ≈5° to 8°). Further, most of the neurons (horizontal, bipolar, amacrine cells) responsible for communicating photic information from the distal photoreceptors to the ipRGCs form a high-density annulus in the macula surrounding the fovea (Lee et al., 2019; Nasir-Ahmad et al., 2017).

Given these anatomical findings, one might reasonably hypothesize that light incident in the fovea and parafovea would be more "circadian effective" than that same amount and spectrum of light stimulating the retina outside the macula. A few studies have specifically examined the topography and density of ipRGCs (Esquiva et al., 2017; Nasir-Ahmad et al., 2017), but none of these neuroanatomical studies have actually characterized the distribution of circadian phototransduction neural circuits that include, but are not synonymous with, ipRGCs (Belenky et al., 2003; Grünert et al., 2011; Jusuf et al., 2007; Perez-Leon et al., 2006). Specifically, the S-cone bipolar neurons as well as AII and A18 amacrine neurons have been postulated to interact directly with ipRGCs in circadian phototransduction (Rea et al., 2021). Consequently, one must employ psychophysical studies to begin to develop a model of the distribution and density of circadian phototransduction circuits across the retina.

The present study's two psychophysical experiments were designed to systematically investigate, for two different spectra, whether the spatial distribution of luminous stimuli in the environment differentially affected nocturnal melatonin suppression, despite being matched for *spectrally weighted corneal irradiance*. Two spatial distributions were employed, one where the luminous stimulus was presented On-axis (along the line of sight) and one where the luminous stimulus was comprised of two luminous elements presented Off-axis (laterally displaced). Two narrowband LED light sources, blue ($\lambda_{max} = 451$ nm) for the first experiment and green ($\lambda_{max} = 522$ nm) for the second experiment, were used for both the On-axis and the Off-axis spatial distributions. In the wake of psychophysical evidence implicating spatial distribution of the light as an important circadian factor (Gaddy et al., 1992), and given the greater density of photoreceptors and neurons in the central retina (fovea plus parafovea) (Nasir-Ahmad et al., 2017; Watson, 2014; Wells-Gray et al., 2016), we hypothesized that melatonin suppression would be greater for the On-axis spatial distribution than for the Off-axis spatial distribution at the same spectrally weighted corneal irradiance, for both light sources (blue and green).

A better understanding of the spatial sensitivity of the human circadian system to photic stimulation is important for providing (1) the most effective lighting used for "bright light therapy" in clinical applications and (2) the best way to install and operate indoor lighting for architectural spaces.

2. Methods

2.1. Participants

Potential participants were recruited via personal referrals, word of mouth, and lists of participants from our previous studies. All potential participants were pre-screened for major health problems such as bipolar disorder, seasonal depression, cardiovascular disease, diabetes, and high blood pressure. Potential participants were excluded from the experiment if they: (1) were taking over-the-counter melatonin or prescription medications such as blood pressure medicine, antidepressants, sleep medicine, or beta-blockers, (2) reported eye diseases such as cataracts or glaucoma, (3) were identified by the study team as having color vision deficiency according to Ishihara color blindness tests (Ishihara, 1960), (4) scheduled or had undertaken transmeridian travel over the course of the study, (5) were shift workers or had worked rotating shifts in the past 3 months, and (6) were extreme chronotypes (Roenneberg et al., 2003) as shown by the Munich Chronotype Questionnaire scores of less than 2 points (slightly early) or greater than 4 points (slightly late). To maintain a stable circadian melatonin rhythm, all participants were required to follow a consistent sleep–wake schedule during the week leading up to each experimental session, with bedtimes no later than 23:00 and wake times no later than 07:30. Given that all participants were either attending school or full-time workers, their sleep schedules were presumed to be regular throughout the duration of the study. Dim light melatonin onset (DLMO) data were not collected for the present experiment to avoid the added expense and burden on experimenters and participants. Rather, we imposed consistent sleep schedules on the participants the week prior to the study and during the two study weeks. This approach has been successful in our laboratory for ensuring that saliva samples for melatonin assay are always collected after what was or would have been DLMO (Figueiro et al., 2013; Figueiro and Rea, 2012). Participants were also asked to refrain from caffeine and alcohol consumption 12 h prior to the beginning of each experimental session. None of the participants reported difficulties in complying with the sleep schedule or the caffeine and alcohol restrictions over the course of the study. The study was conducted in accordance with the Declaration of Helsinki (World Medical Association, 2000) and was approved by the Institutional Review Board at Rensselaer Polytechnic Institute. Informed
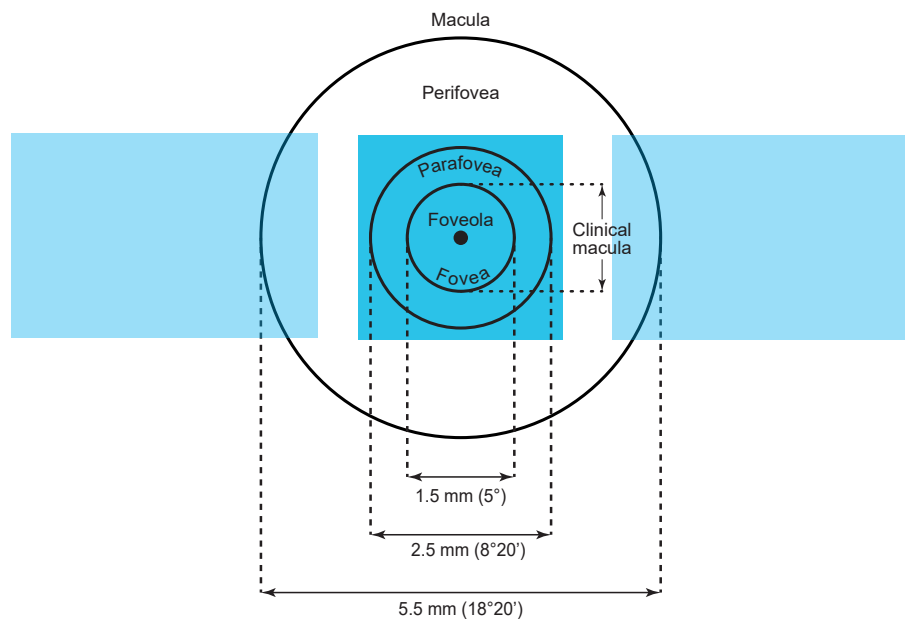

Fig. 1. Schematic projection of the off-axis (shown in light blue) and on-axis (shown in dark blue) distributions with respect to the macula and its subareas. (Adapted from an illustration by Zyxwv99, Wikimedia Commons, distributed under a CC-BY 4.0 license.) (For interpretation of the references to color in this figure legend, the reader is referred to the Web version of this article.)

consent was obtained from all study participants.

The study included two experiments of 3 weeks each, with Experiment 1 commencing March 2019 and Experiment 2 commencing February 2020. Twenty-five adults participated in Experiment 1 (mean age = 34.0 years [SD 15.5]; 13 females; mean chronotype score = 2.7 [SD 1.2]) and 15 adults participated in Experiment 2 (mean age = 43.0 years [SD 12.6]; 12 females; mean chronotype score = 2.7 [SD 1.1]).

2.2. Experimental conditions

Participants from both experiments reported to the laboratory on three consecutive Friday nights. This allowed for a washout period between the three experimental conditions, including a dim-light control condition that served as the baseline for calculating light-induced melatonin suppression. For each experiment, the participants were randomly divided into three equal groups, and each group was exposed to a single experimental condition during a Friday night session according to a planned, counter-balanced order.

During Experiment 1, participants were exposed to the blue light source (λ_{max} = 451 nm, Fig. 2), whereas during Experiment 2 participants were exposed to the green light source (λ_{max} = 522 nm, Fig. 2). Spectral irradiance measurements of the two light sources were taken using a spectrometer (Model USB650, Ocean Optics, Winter Park, FL, USA). The blue light was provided by an RGB (primarily B) color-tunable, LED linear accent module (model G2, Ketra, Austin, TX) driven by a satellite link controller (model N3, Ketra Inc. Austin, TX) with a touchpad interface (model X1, Ketra). The green light was provided by a Kaper green light module (model L16-0079 GR, Kaper II Inc. Kelso, WA).

In both experiments, two spatial distributions of light (On-axis and Off-axis) were delivered, in turn, to participants from a diffuse, luminous element of a 56 cm × 13 cm (22 in × 5 in) luminaire. The luminaires were placed on a desk surface; the center of the luminaire was 80 cm (31.5 in) from the participant's eyes when his/her chin was positioned in a fixed rest (Fig. 3). Discomfort glare on the de Boer scale (de Boer, 1967) for the On-axis intervention, calculated following Bullough et al. (Alliance for Solid-State Illumination Systems and Technologies (ASSIST), 2011), was determined to be 6.9 (satisfactory) and 5.5 (acceptable) for the blue light source and the green light source, respectively.

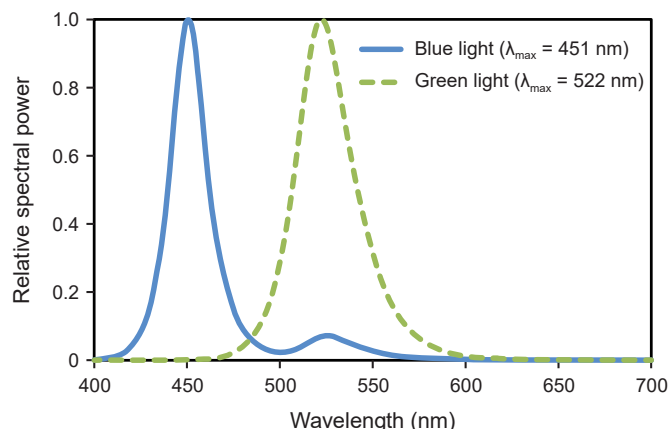To control delivery of the prescribed light level for both spatial

Fig. 2. Relative spectral power distributions of the narrowband blue light source (λ_{max} = 451 nm) and the green light source (λ_{max} = 522 nm) employed for the two spatial distributions, On-axis and Off-axis. Note that the relative spectral power distribution of the blue light source was not determined by a single LED type (B); rather, the control system only minimized flux from the other two LED types (R and G) in the luminaire. (For interpretation of the references to color in this figure legend, the reader is referred to the Web version of this article.)

distributions, a participant was required to perform a simple On-axis visual task while his/her chin was positioned in a fixed rest (Fig. 3). Specifically, the participant was instructed to continuously fixate on a low-power LED light and tally the number of times it switched color from white to red using a hand-held counter. The fixation light was not needed on the dim-light control night. For both the blue and the green light stimuli, the On-axis spatial distribution was comprised of a 13 cm × 13 cm (5 in × 5 in) luminous element. At the prescribed viewing distance, this On-axis luminous square subtended a solid angle (Ω) of 0.027 steradians at the participant's eyes (9.4° × 9.4°, horizontal [h] × vertical [v]). Both the blue and the green Off-axis spatial distributions were comprised of two 19 cm × 13 cm (7.5 in × 5 in) luminous rectangles, with their respective centers laterally displaced by ± 14° from the fixation point (Fig. 3; see Fig. 1). At the prescribed viewing distance, each of these luminous rectangles subtended solid angles of 0.039 steradians at the participant's eyes (12.7° [h] × 9.4° [v]).

For both experiments, the respective light source was calibrated to deliver the same spectrally weighted irradiance at the participants' eyes for the two spatial distributions. There are a variety of ways to characterize the spectrally weighted irradiance. All of the characterizations presented in Table 1 were determined from the relative spectral power distributions of the blue and green LEDs (see Fig. 2) and levels recorded by an illuminance meter (Model X-91, Gigahertz-Optik, Haverhill Rd, Amesbury, MA, USA) with the tripod-mounted, cosine-corrected sensor positioned where the bridge of the participant's nose was expected to be during the experiment. Table 2 shows the corresponding α-opic irradiances, calculated using the CIE S 026 α-opic Toolbox (v1.049) (Commission Internationale de l'Éclairage, 2018, 2020).

2.3. Protocol

For each experiment, over the course of three experimental sessions, participants arrived at the laboratory before 23:30 and remained in dim light (<5 lx at the eyes) for 30 min, after which they experienced 60 min of one of the two lighting conditions (On-axis or Off-axis) or the dim-light control (Fig. 4).

Three saliva samples were collected from each participant during each session. The first sample (S1) was taken immediately before the beginning of the light intervention and after a 30-min dim light exposure; the two remaining samples (S2 and S3) were taken thereafter at 30-min intervals. At 01:00, participants were free to leave the laboratory. This experimental protocol has been previously employed and specified in Nagare, Rea, et al. (2019a).

Saliva samples (1 ml) were collected using the Salivette system (Sarstedt, Nümbrecht, DE) which has been successfully employed in prior studies at our lab (Figueiro et al., 2009; Figueiro et al., 2011; Nagare, Rea, et al., 2019b), wherein the participant chews on a plain cotton cylinder for 1–2 min (not timed individually) that was immediately placed in a test tube, centrifuged for 5 min at 1000 g, and frozen (−20 °C). The frozen samples from each session were assayed in a single batch using melatonin radioimmunoassay kits (Catalog number 79-MEHLU-R100, Direct Melatonin RIA, ALPCO, Salem, NH, USA). The sensitivity of the saliva sample assay was reported to be 0.3 pg ml^{-1} and the intra- and inter-assay coefficients of variability were 11–14% and 14–17%, respectively. During each session, the participants refrained from consuming any food and were allotted a 10-min window to drink water, following each saliva sample time. Periodic visual monitoring and performance checks on the fixation light counters were carried out on each study night to ensure compliance with the instructed gaze direction and that the study participants did not close their eyes during the light exposure. Two participants from Experiment 1 and one participant from Experiment 2 failed to follow the study protocol (trouble keeping eyes open, unacceptable fixation count) and were excluded from the analyses. Two participants from Experiment 1 withdrew their participation from the study due to illness.

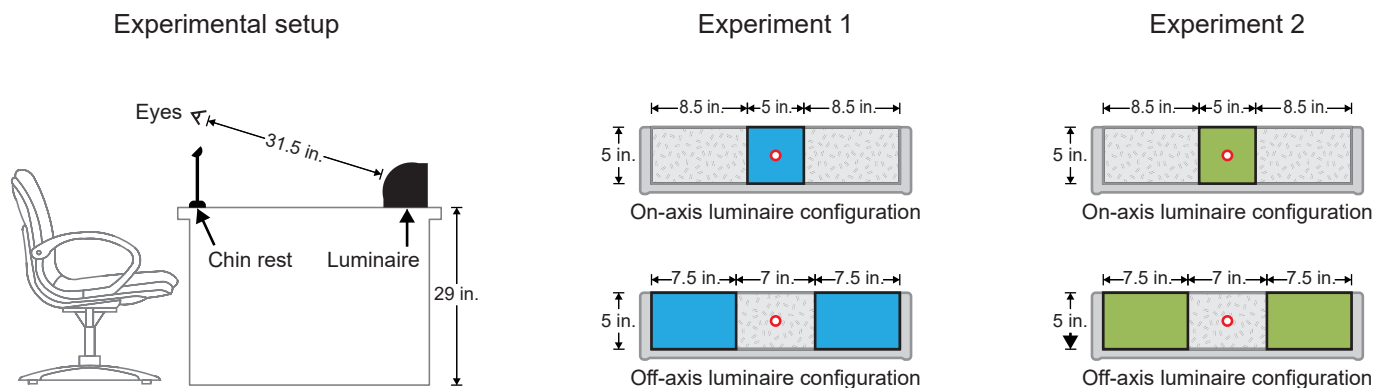During each experimental session, participants' pupil areas were

Fig. 3. The layout of the desktop luminaires in both Experiment 1 (blue) and Experiment 2 (green) with respect to the participants' eyes during the experiment (left), and the two spatial distributions of the luminous stimuli when delivering the On-axis and Off-axis interventions (right). The regions highlighted in blue and green depict the luminous areas. The circle shown in the center of the luminaires represents the suspended, dynamic low-power LEDs that were used to maintain fixation (see Protocol). (For interpretation of the references to color in this figure legend, the reader is referred to the Web version of this article.)

Table 1
Photometric characteristics of the luminous stimuli.

Experimental condition	Photopic illuminance (lx)	Melanopic equivalent daylight (D65) illuminance	Circadian light 2.0 [a]	Circadian stimulus [a]
Experiment 1 (Blue light; On-/Off-axis)	26	136	274	0.30
Experiment 2 (Green light; On-/Off-axis)	287	251	256	0.28

[a] Circadian light 2.0 and circadian stimulus are calculated from the updated model of circadian phototransduction (Rea et al., 2021).

measured once (after the second saliva sample, S2) during the lighting intervention. Each participant was required, in turn, to hold a reference scale (a ruler) directly beneath their dominant eye while a 15-s video clip was recorded using a digital video camcorder (model DCR-TRV140, SONY Electronics, Minato, Tokyo, Japan). Average pupil area was estimated from five single-frame samples of the video clip using an open-source web application (Pixel Ruler, MIOPlanet Technologies, Rimouski, PQ, Canada). Pupil area could not be determined for two participants in Experiment 1 due to insufficient resolution of the recorded digital images.

For both experiments, on the dim-light control night, participants were seated at the table that held the (dark) luminaire (see Fig. 3) but were free to operate their personal electronic devices (i.e., computers, tablets, cell phones, etc.). To ensure the control condition was experienced in "circadian darkness," all electronic devices were dimmed and covered with orange filters (Roscolux #21 golden amber, Rosco Laboratories, Stamford, CT, USA) that eliminated all optical radiation <525 nm. Thus, the dim settings and the orange filter prevented participants from receiving *any* circadian-effective light during the dim-light control condition (Nagare et al., 2019a).

2.4. Data analysis

For each participant, melatonin suppression was determined by comparing the raw melatonin levels collected during the dim light control night to those collected at the corresponding times on each lighting intervention night (see Fig. 4). For each session, melatonin concentrations measured from S2 and S3 were first normalized to S1, and the melatonin suppression values for 30 and 60 min were then calculated using the following formula:

$$Suppression = 1 - \left(\frac{M_n}{M_d}\right) \times 100 \qquad (1)$$

where M_n is the normalized melatonin concentration at each time on respective intervention nights and M_d is the normalized melatonin concentration at each time on the dim light control night.

Melatonin suppression data from the two experiments were analyzed separately using general linear model (GLM) repeated measures ANOVA, with lighting distribution (On-axis vs. Off-axis), and exposure duration (30-min vs. 60-min) serving as the within-subjects factors. The ANOVA was performed using SPSS statistical software (SPSS version 26, IBM, Armonk, NY, USA). All results were considered to be statistically significant if the resulting p value was <0.05. There were no missing
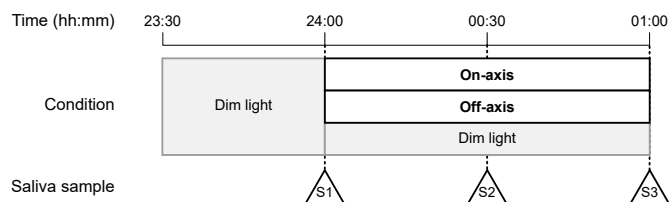

Fig. 4. Experimental protocol for both Experiment 1 (blue light) and Experiment 2 (green light), bold, showing the salivary melatonin sample times (S1, S2, and S3). The order of presentation for the On-axis, Off-axis and Dim-light control conditions was counterbalanced across three groups.

Table 2
The α-opic irradiances for all experimental conditions calculated using the CIE S 026 α-opic Toolbox (v1.049).

Experimental condition	S-cone-opic irradiance W. m⁻²	M-cone-opic irradiance W. m⁻²	L-cone-opic irradiance W. m⁻²	Rhodopic irradiance W. m⁻²	Melanopic irradiance W. m⁻²
Experiment 1 (Blue light; On-/Off-axis)	0.24	0.07	0.05	0.16	0.18
Experiment 2 (Green light; On-/Off-axis)	0.02	0.49	0.41	0.45	0.33

Source for calculations: Commission Internationale de l'Éclairage (2020).

melatonin data from Experiment 1. There were four missing melatonin data points from Experiment 2 across three participants due to a lack of saliva retrieved for assays (two for S2 On-axis intervention and two for S3 On-axis intervention). Preliminary melatonin data quality control revealed that melatonin levels prior to energizing the lights (S1) were always above the sampling threshold for detection 0.3 pg ml^{-1} (Catalog number 79-MEHLU-R100, Direct Melatonin RIA, ALPCO, Salem, NH, USA); for Experiment 1 the mean concentration was 15.8 pg ml^{-1} (SD 11.4) and for Experiment 2 the mean concentration was 12.8 pg ml^{-1} (SD 11.2). Plots depicting raw melatonin data are provided in Supplemental Fig. S1. A secondary ANOVA was performed with the pupil area as the dependent variable, and lighting distribution as the independent variable.

3. Results

Experiment 1 (blue light): The ANOVA revealed a significant main effect of distribution ($F_{1,20} = 21.90$, $p < 0.001$; Fig. 5a), wherein melatonin suppression was significantly greater for the On-axis condition (mean = 27.0% [SD 19.5]) compared to the Off-axis condition (mean = 8.1% [SD 29.2]). This suggests that the central retina (fovea plus parafovea) is much more sensitive than the more peripheral retina at the same spectrally weighted irradiance at the eye for light-induced melatonin suppression.

A significant main effect of light exposure duration was observed ($F_{1,20} = 21.25$, $p < 0.001$; Fig. 5b), wherein greater melatonin suppression was observed following the 1-h exposure duration (mean ± SD = 25.4 [SD 26.1]) compared to the 0.5-h exposure duration (mean = 9.7% [SD 24.5]). The two-way interaction between the independent variables was not statistically significant.

The secondary ANOVA revealed that the main effect of lighting distribution on pupil area was not significant. The mean pupil areas for the On-axis and Off-axis blue light conditions were 6.14 mm^2 (SD 2.97) and 6.84 mm^2 (SD 3.79), respectively.

Experiment 2 (green light): The ANOVA revealed a significant main effect of distribution ($F_{1,10} = 40.26$, $p < 0.001$; Fig. 5c), wherein melatonin suppression was significantly greater for the On-axis condition (mean = 29.0% [SD 14.8]) compared to the Off-axis condition (mean = 14.5% [SD 17.6]). This finding is consistent with the findings from the first experiment.

The effect of light exposure duration on melatonin suppression was not observed ($F_{1,10} = 1.67$, $p = 0.23$; Fig. 5d), wherein melatonin suppression following the 1-h exposure duration (mean 25.8% [SD17.8]) was not significantly greater than the melatonin suppression following the 0.5-h exposure duration (mean = 16.6% [SD 16.9]). The two-way interaction between the independent variables was not statistically significant.

The secondary ANOVA revealed that the main effect of lighting distribution on pupil area was not significant. The mean pupil areas for the On-axis and Off-axis green light conditions were 5.16 mm^2 (SD 1.40) and 5.77 mm^2 (SD 1.55), respectively.

4. Discussion

The primary goal of the present study was to better understand how the spatial distribution of luminous stimuli affected nocturnal melatonin suppression. Implicitly, the spectrally weighted irradiance at the eyes should rectify all spatial distributions into a single, predictive photometric quantity. The present results show this assumption is not valid.

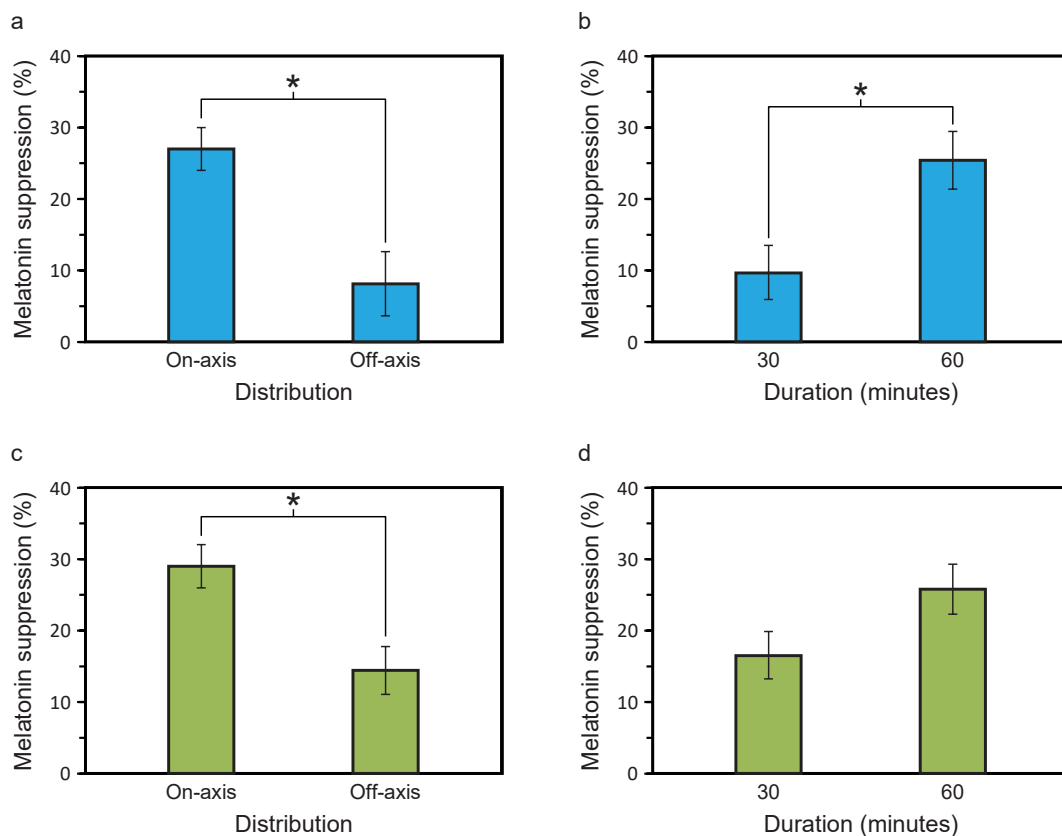Two spatial distributions producing the same spectrally weighted

Fig. 5. Mean melatonin suppression, compared to the dim-light control condition, for (a) the two blue light spatial distribution profiles combined across duration, (b) the two blue light duration profiles combined across distributions, (c) the two green light spatial distribution profiles combined across duration, (d) the two green light duration profiles combined across distributions. The error bars represent standard error of the mean (SEM) and the asterisks represent statistical significance ($p < 0.001$). (For interpretation of the references to color in this figure legend, the reader is referred to the Web version of this article.)

irradiance at the eyes led to significantly different levels of nocturnal melatonin suppression. For the first experiment, the On-axis blue light stimulus targeting the central retina (fovea plus parafovea) was about three times more effective than the photometrically and spectrally matched Off-axis blue light stimulus at the eyes targeting the more peripheral retina. For the second experiment, the On-axis green light stimulus targeting the central retina was about two times more effective than the photometrically and spectrally matched Off-axis green light stimulus. These findings suggest that most of the phototransduction mechanisms leading to light-induced melatonin suppression are largely due to phototransduction circuits in the central retina or the macular region.

The results presented here may seem inconsistent with those reported in an earlier study by Adler et al. (1992), wherein 12 healthy subjects were treated to bright light exposure (1000 lx) under two spatial lighting scenarios: central and laterally peripheral, but failed to report a significant difference in melatonin levels between the two lighting conditions. In that study however, the "central" light source was offset by 5° from participant's line of gaze, as they were instructed to look at a television screen and not directly at the light source positioned next to it. Thus, both stimuli in the Adler et al. study were probably presented outside the parafovea.

The lower circadian efficacy of Off-axis stimulus may, at least in part, be attributed to the greater density of RGCs and cone photoreceptors in the central retina (Curcio and Allen, 1990; Curcio et al., 1990; Packer et al., 1989; van der Merwe et al., 2018). For instance, based upon the spatial distribution of various retinal components by Patney et al. (2016), it was estimated that average density for the RGCs within the central 5° visual field is ≈ 17,900 cells per square millimeter. The average density for RGCs in the perifoveal region and beyond, drops by a factor of 2.6 to ≈6800 cells per square millimeter within an 8°–20° visual field. As a simple model, assuming direct translation of the decreased perifoveal density of RGCs also reflects the drop in density of ipRGCs, a greater than two-fold drop in the ipRGCs density is consistent with a greater than two-fold drop in reported melatonin suppression for the Off-axis sources compared to the On-axis source.

It was observed that even though average melatonin suppression following the On-axis exposures to the blue light (27%) and green light conditions (29%) from the two independent experiments was quite similar, melatonin suppression following the Off-axis exposure to the green light condition (15%) was almost twice that of the Off-axis suppression for the blue light condition (8%). The present experiments were not designed to explore whether the circadian system's spectral sensitivity as characterized by nocturnal melatonin suppression varies with retinal eccentricity; however, these data indicate an interesting research avenue to pursue in a follow-up study.

A note on the possible effects of discomfort glare (Boyce, 2014; Rea, 2000) and retinal illuminance from the luminous stimuli is warranted. Discomfort glare can result in gaze aversion or squinting, particularly to luminous stimuli viewed On-axis and dominated by short wavelengths (Albilali and Dilli, 2018; Matynia et al., 2012). Since there was no statistical difference in suppression between the blue and green light sources and because the luminous stimuli presented to the central retina (fovea plus parafovea) were associated with greater, rather than lower, melatonin suppression across both the spectra, the discomfort glare estimate determined prior to conducting the experiment ("satisfactory" or "acceptable") was apparently valid. In short, discomfort glare was unlikely to be a factor in the present study. Further, because the pupil area did not differ significantly between the On-axis (6.14 mm^2 for the blue and 5.16 mm^2 for the green light) and Off-axis luminous stimuli (6.84 mm^2 for the blue and 5.77 mm^2 for the green light), it is unlikely that retinal illuminance entering the eyes from the two spatial distributions differentially affected the results of the experiments.

A few limitations to the study are worth noting. First, there were more female than male participants (25 females, 15 males) across the two experiments. Past studies have reported no differences in chronotype and sleep characteristics with respect to sex (Giannotti et al., 2002; Russo et al., 2007). Further, Nathan et al. (2000) showed that nighttime melatonin suppression values were similar across healthy men and women following 1-h exposure at five white light levels (0–3000 lx). Therefore, it seems unlikely that having more female participants than male participants in the study would have affected the results. Second, daily light exposures prior to and between in-laboratory sessions were not controlled. In principle, participants could have had somewhat different photic histories prior to a given session (Chang et al., 2011; Smith et al., 2004), but these differences would have been small because all were full-time employees or students with regular schedules. Therefore, and based upon previous studies from our laboratory using the same protocol (Nagare, Plitnick, et al., 2019b; Nagare, Rea, et al., 2019a, 2019b), it was deemed safe to assume that any possible differences in photic history, both between and within participants, would be small and uncorrelated with any of the independent variables, thereby helping to insure the statistical inferences would not be compromised.

Lastly, the study was primarily designed to investigate the acute effect of light exposure on melatonin suppression, and the participants' circadian phase was not assessed. However, melatonin levels prior to energizing the lights (S1) were always ≥ 3 pg ml^{-1}, the commonly accepted threshold for salivary dim-light melatonin onset (Lewy, 2007), and the sampling time of the salivary melatonin assays was held constant across all experimental conditions for all study participants. Given this protocol, any within-subjects variability in the absolute melatonin concentrations during the sampling times would have been small and random and would not, therefore, compromise the statistical inferences.

From a practical perspective, these results are quite intriguing. If the circadian phototransduction mechanisms are concentrated in the central retina (angular diameter ⪅ 8°), then interventions such as light boxes placed peripherally to the line of sight (Off-axis) would be relatively ineffective in stimulating the human circadian system unless they provided particularly high irradiance at the eye. Thus, it is important that personalized tabletop fixtures illuminating desks and work surfaces be positioned closer to the occupant's line of sight to ensure a high circadian-effective photic stimulus during the daytime. The same principle can also be used to substantially lower light-induced melatonin suppression among night-shift workers by positioning bright desktop luminaires far from the occupant's line of sight. However, nighttime use of self-luminous displays (e.g., iPad 3rd gen, with On-axis spatial extent of 13° [h] × 16° [v] from a viewing distance of 76.2 cm) could be particularly disruptive because majority of the light reaching the retina would be concentrated in the macular region.

The potential practical implications of the results presented will hopefully encourage subsequent translational research to more precisely determine the spatial distribution of circadian phototransduction circuits in the retina and how practical light-delivery apparatus can be implemented in the workplace. In the meantime, we should all try to reduce the use of On-axis light sources such as self-luminous displays in the home at night to prevent circadian disruption.

Data availability statement

The data sets generated during and/or analyzed during the study are available from the corresponding author on reasonable request.

Declaration of competing interest

The author(s) have no potential conflicts of interest with respect to the research, authorship, and/or publication of this article.

CRediT authorship contribution statement

Rohan Nagare: Conceptualization, Formal analysis, Investigation, Data curation, Writing – original draft. **Mark S. Rea:** Supervision, Formal analysis, Methodology, Writing – review &; editing. **Mariana G.**

Appendix A. Supplementary data

Supplementary data to this article can be found online at https://doi.org/10.1016/j.nbscr.2021.100071.

References

Adler, J.S., Kripke, D.F., Loving, R.T., Berga, S.L., 1992. Peripheral vision suppression of melatonin. J. Pineal Res. 12 (2), 49–52. https://doi.org/10.1111/j.1600-079x.1992.tb00025.x.

Albilali, A., Dilli, E., 2018. Photophobia: when light hurts, a review. Curr. Neurol. Neurosci. Rep. 18 (9), 62. https://doi.org/10.1007/s11910-018-0864-0.

Alliance for Solid-State Illumination Systems and Technologies (Assist), 2011. A method for estimating discomfort glare from exterior lighting systems. Assist Recommends 9 (1), 1–7. https://www.lrc.rpi.edu/programs/solidstate/assist/pdf/AR-Discomfort Glare.pdf.

Belenky, M.A., Smeraski, C.A., Provencio, I., Sollars, P.J., Pickard, G.E., 2003. Melanopsin ganglion cells receive bipolar and amacrine cell synapse. J. Comp. Neurol. 460, 380–393. https://doi.org/10.1002/cne.10652.

Boyce, P.R., 2014. Human Factors in Lighting, third ed. CRC Press, Boca Raton, FL.

Brainard, G.C., Hanifin, J.P., Greeson, J.M., Byrne, B., Glickman, G., Gerner, E., Rollag, M.D., 2001. Action spectrum for melatonin regulation in humans: evidence for a novel circadian photoreceptor. J. Neurosci. 21 (16), 6405–6412. https://doi.org/10.1523/JNEUROSCI.21-16-06405.2001.

Bumsted, K., Hendrickson, A., 1999. Distribution and development of short-wavelength cones differ between Macaca monkey and human fovea. J. Comp. Neurol. 403 (4), 502–516. https://www.ncbi.nlm.nih.gov/pubmed/9888315.

Calkins, D.J., 2001. Seeing with S cones. Prog. Retin. Eye Res. 20 (3), 255–287. https://doi.org/10.1016/s1350-9462(00)00026-4.

Chang, A.M., Scheer, F.A., Czeisler, C.A., 2011. The human circadian system adapts to prior photic history. J. Physiol. 589 (Pt 5), 1095–1102. https://doi.org/10.1113/jphysiol.2010.201194.

Commission Internationale de l'Éclairage, 2018. *CIE system for metrology of optical radiation for ipRGC-influenced responses to light,* CIE S 026/E:2018. Commission Internationale de l'Éclairage. http://cie.co.at/publications/cie-system-metrology-optical-radiation-iprgc-influenced-responses-light-0.

Commission Internationale de l'Éclairage, 2020. *The α-opic Toolbox* (v1.049, 2020/03/26. Commission Internationale de l'Éclairage, Vienna. https://bit.ly/33YM9Rh.

Curcio, C.A., Allen, K.A., 1990. Topography of ganglion cells in human retina. J. Comp. Neurol. 300 (1), 5–25. https://doi.org/10.1002/cne.903000103.

Curcio, C.A., Sloan, K.R., Kalina, R.E., Hendrickson, A.E., 1990. Human photoreceptor topography. J. Comp. Neurol. 292 (4), 497–523. https://doi.org/10.1002/cne.902920402.

de Boer, J.B., 1967. Visual perception in road traffic and the field of vision of the motorist. In: de Boer, J.B. (Ed.), Public Lighting. Philips Technical Library, Eindhoven, The Netherlands, pp. 11–96.

Esquiva, G., Lax, P., Perez-Santonja, J.J., Garcia-Fernandez, J.M., Cuenca, N., 2017. Loss of melanopsin-expressing ganglion cell subtypes and dendritic degeneration in the aging human retina. Front. Aging Neurosci. 9, 79. https://doi.org/10.3389/fnagi.2017.00079.

Figueiro, M.G., Bierman, A., Bullough, J.D., Rea, M.S., 2009. A personal light-treatment device for possibly improving sleep quality in the elderly: dynamics of nocturnal melatonin suppression at two exposure levels. Chronobiol. Int. 26 https://doi.org/10.1080/07420520902927809.

Figueiro, M.G., Bierman, A., Rea, M.S., 2013. A train of blue light pulses delivered through closed eyelids suppresses melatonin and phase shifts the human circadian system. Nat. Sci. Sleep 5, 133–141. https://doi.org/10.2147/NSS.S52203.

Figueiro, M.G., Lesniak, N.Z., Rea, M.S., 2011. Implications of controlled short-wavelength light exposure for sleep in older adults. BMC Res. Notes 4, 334. https://doi.org/10.1186/1756-0500-4-334.

Figueiro, M.G., Rea, M.S., 2012. Preliminary evidence that light through the eyelids can suppress melatonin and phase shift dim light melatonin onset. BMC Res. Notes 5 (1), 221. https://doi.org/10.1186/1756-0500-5-221.

Gaddy, J.R., Edelson, M., Stewart, K., Brainard, G.C., Rollag, M.D., 1992. Possible retinal spatial summation in melatonin suppression. In: Holick, M.F., Klingman, A.M. (Eds.), Biologic Effects of Light. Walter de Gruyter, New York, pp. 196–204.

Giannotti, F., Cortesi, F., Sebastiani, T., Ottaviano, S., 2002. Circadian preference, sleep and daytime behaviour in adolescence. J. Sleep Res. 11 (3), 191–199. https://doi.org/10.1046/j.1365-2869.2002.00302.x.

Grünert, U., Jusuf, P.R., Lee, S.C.S., Nguyen, D.T., 2011. Bipolar input to melanopsin containing ganglion cells in primate retina. Vis. Neurosci. 28 (1), 39–50. https://doi.org/10.1017/S095252381000026X.

Hannibal, J., Christiansen, A.T., Heegaard, S., Fahrenkrug, J., Kiilgaard, J.F., 2017. Melanopsin expressing human retinal ganglion cells: subtypes, distribution, and intraretinal connectivity. J. Comp. Neurol. 525 (8), 1934–1961. https://doi.org/10.1002/cne.24181.

Ishihara, S., 1960. Tests for Colour-Blindness, 15 ed. H. K. Lewis, London.

Jusuf, P.R., Lee, S.C.S., Hannibal, J., Grünert, U., 2007. Characterization and synaptic connectivity of melanopsin-containing ganglion cells in the primate retina. Eur. J. Neurosci. 26 (10), 2906–2921. https://doi.org/10.1111/j.1460-9568.2007.05924.x.

Khalsa, S.B., Jewett, M.E., Cajochen, C., Czeisler, C.A., 2003. A phase response curve to single bright light pulses in human subjects. J. Physiol. 549 (Pt 3), 945–952. https://doi.org/10.1113/jphysiol.2003.040477.

Kolb, H., Nelson, R., Ahnelt, P., Ortuño-Lizarán, I., Cuenca, N., 2020. The architecture of the human fovea. In: Kolb, H., Nelson, R., Fernandez, E. (Eds.), Webvision: the Organization of the Retina and Visual System, 2020. University of Utah Health Sciences Center. https://www.ncbi.nlm.nih.gov/books/NBK554706/.

Lee, S.C.S., Martin, P.R., Grünert, U., 2019. Topography of neurons in the rod pathway of human retina. Invest. Ophthalmol. Vis. Sci. 60 (8), 2848–2859. https://doi.org/10.1167/iovs.19-27217.

Lewy, A.J., 2007. Melatonin and human chronobiology. Cold Spring Harbor Symp. Quant. Biol. 72, 623–636. https://doi.org/10.1101/sqb.2007.72.055.

Matynia, A., Parikh, S., Chen, B., Kim, P., McNeill, D.S., Nusinowitz, S., Evans, C., Gorin, M.B., 2012. Intrinsically photosensitive retinal ganglion cells are the primary but not exclusive circuit for light aversion. Exp. Eye Res. 105, 60–69. https://doi.org/10.1016/j.exer.2012.09.012.

Nagare, R., Plitnick, B., Figueiro, M.G., 2019a. Does the iPad Night Shift mode reduce melatonin suppression? Light. Res. Technol. 51 (3), 373–383. https://doi.org/10.1177/1477153517748189.

Nagare, R., Plitnick, B., Figueiro, M.G., 2019b. Effect of exposure duration and light spectra on nighttime melatonin suppression in adolescents and adults. Light. Res. Technol. 51 (4), 530–540. https://doi.org/10.1177/1477153518763003.

Nagare, R., Rea, M.S., Plitnick, B., Figueiro, M.G., 2019a. Effect of white light devoid of "cyan" spectrum radiation on nighttime melatonin suppression over a 1-h exposure duration. J. Biol. Rhythm. 34 (2), 195–204. https://doi.org/10.1177/0748730419830013.

Nagare, R., Rea, M.S., Plitnick, B., Figueiro, M.G., 2019b. Nocturnal melatonin suppression by adolescents and adults for different levels, spectra, and durations of light exposure. J. Biol. Rhythm. 34 (2), 178–194. https://doi.org/10.1177/0748730419828056.

Nasir-Ahmad, S., Lee, S.C.S., Martin, P.R., Grünert, U., 2017. Melanopsin-expressing ganglion cells in human retina: morphology, distribution, and synaptic connections. J. Comp. Neurol. 527 (1), 312–327. https://doi.org/10.1002/cne.24176.

Nathan, P.J., Wyndham, E.L., Burrows, G.D., Norman, T.R., 2000. The effect of gender on the melatonin suppression by light: a dose response relationship. J. Neural. Transm. 107 (3), 271–279. https://doi.org/10.1007/s007020050022.

Packer, O., Hendrickson, A.E., Curcio, C.A., 1989. Photoreceptor topography of the retina in the adult pigtail macaque (*Macaca nemestrina*). J. Comp. Neurol. 288 (1), 165–183. https://doi.org/10.1002/cne.902880113.

Patney, A., Salvi, M., Kim, J., Kaplanyan, A., Wyman, C., Benty, N., Luebke, D., Lefohn, A., 2016. Towards foveated rendering for gaze-tracked virtual reality. ACM Trans. Graph. 35 (6), 1–12. https://doi.org/10.1145/2980179.2980246. Article 179.

Perez-Leon, J.A., Warren, E.J., Allen, C.N., Robinson, D.W., Brown, R.L., 2006. Synaptic inputs to retinal ganglion cells that set the circadian clock. Eur. J. Neurosci. 24 (4), 1117–1123. https://doi.org/10.1111/j.1460-9568.2006.04999.x.

Rea, M.S., 2000. IESNA Lighting Handbook: Reference and Application, ninth ed. Illuminating Engineering Society of North America, New York, NY.

Rea, M.S., Nagare, R., Figueiro, M.G., 2021. Modeling circadian phototransduction: retinal neurophysiology and neuroanatomy. Front. Neurosci. 14, 1467. https://doi.org/10.3389/fnins.2020.615305.

Roenneberg, T., Wirz-Justice, A., Merrow, M., 2003. Life between clocks: daily temporal patterns of human chronotypes. J. Biol. Rhythm. 18 (1), 80–90. https://doi.org/10.1177/0748730402239679.

Russo, P.M., Bruni, O., Lucidi, F., Ferri, R., Violani, C., 2007. Sleep habits and circadian preference in Italian children and adolescents. J. Sleep Res. 16 (2), 163–169. https://doi.org/10.1111/j.1365-2869.2007.00584.x.

Smith, K.A., Schoen, M.W., Czeisler, C.A., 2004. Adaptation of human pineal melatonin suppression by recent photic history. J. Clin. Endocrinol. Metab. 89 (7), 3610–3614. https://doi.org/10.1210/jc.2003-032100.

St Hilaire, M.A., Gooley, J.J., Khalsa, S.B., Kronauer, R.E., Czeisler, C.A., Lockley, S.W., 2012. Human phase response curve to a 1 h pulse of bright white light. J. Physiol. 590 (Pt 13), 3035–3045. https://doi.org/10.1113/jphysiol.2012.227892.

Thapan, K., Arendt, J., Skene, D.J., 2001. An action spectrum for melatonin suppression: evidence for a novel non-rod, non-cone photoreceptor system in humans. J. Physiol. 535, 261–267. https://doi.org/10.1111/j.1469-7793.2001.t01-1-00261.x.

van der Merwe, I., Lukats, A., Blahova, V., Oosthuizen, M.K., Bennett, N.C., Nemec, P., 2018. The topography of rods, cones and intrinsically photosensitive retinal ganglion cells in the retinas of a nocturnal (Micaelamys namaquensis) and a diurnal (Rhabdomys pumilio) rodent. PloS One 13 (8), e0202106. https://doi.org/10.1371/journal.pone.0202106.

Watson, A.B., 2014. A formula for human retinal ganglion cell receptive field density as a function of visual field location. J. Vis. 14 (7) https://doi.org/10.1167/14.7.15, 15-15.

Wells-Gray, E.M., Choi, S.S., Bries, A., Doble, N., 2016. Variation in rod and cone density from the fovea to the mid-periphery in healthy human retinas using adaptive optics scanning laser ophthalmoscopy. Eye 30 (8), 1135–1143. https://doi.org/10.1038/eye.2016.107.

World Medical Association, 2000. World Medical Association Declaration of Helsinki: ethical principles for medical research involving human subjects. J. Am. Med. Assoc. 284 (23), 3043–3045. https://doi.org/10.1001/jama.284.23.3043.

Zeitzer, J.M., Dijk, D.J., Kronauer, R.E., Brown, E.N., Czeisler, C.A., 2000. Sensitivity of the human circadian pacemaker to nocturnal light: melatonin phase resetting and suppression. J. Physiol. 526 (Pt3), 695–702. https://doi.org/10.1111/j.1469-7793.2000.00695.x.